Reducing Cyclic Variability While Regulating Combustion Phasing in a Four-Cylinder HCCI Engine

Erik Hellström, *Member, IEEE*, Jacob Larimore, *Student Member, IEEE*, Shyam Jade, *Student Member, IEEE*, Anna G. Stefanopoulou, *Fellow, IEEE*, and Li Jiang

***Abstract*— The cyclic variability (CV) at late phasing conditions in autoignition engines with high residuals limits the operating range of such advanced combustion strategies. A model has been recently proposed by the authors that captures the experimental observations of CV in lean autoignition combustion in a single-cylinder engine. The model is here tuned to multicylinder engine data and is used to design controllers that reduce the CV. The dynamics are only stable for certain amounts of residual gas. At late phasing, with low amounts of residual gas, a cascade of period-doubling bifurcations occur leading to seemingly chaotic behavior. The deterministic dynamics are also mixed with significant levels of noise in the residual gas fraction. The approach to reduce CV is to control the fuel injection timing, which is an effective way of influencing the combustion phasing in the individual cylinders, with feedback from the combustion phasing. A PI controller and a reduced-order linear quadratic Gaussian (LQG) controller are designed and evaluated in experiments. Integral action is utilized for maintaining the average combustion phasing between open loop and closed loop, which is shown to be essential for a proper evaluation because of the high sensitivity of CV on the combustion phasing close to unstable operation. A quantitative analysis of the experimental results show that CV is notably reduced for various levels of residual gas fraction at one speed and load. The standard deviation of the combustion phasing is reduced by 17% on average over the open-loop behavior, which results in a 15% smaller coefficient of variation of the indicated work.**

***Index Terms*— Bifurcation, internal combustion engines, linear feedback control systems, nonlinear dynamical systems, stability.**

I. Introduction

COMPARED to more traditional combustion concepts, controlled autoignition combustion), also called homogeneous charge compression ignition (HCCI), with a high level of residual gas promises a more clean and efficient operation [1]. At the same time, the operating range for this type of combustion is narrower and transient control is more challenging, which limits its use in commercial applications. Cyclic variability (CV) is a major factor that limits the operating range [2], [3] and complicates load transients [4], [5].

Manuscript received October 21, 2012; accepted June 15, 2013. Manuscript received in final form June 24, 2013. Date of publication July 15, 2013; date of current version April 17, 2014. This work was supported in part by the Department of Energy under Award DE-EE0003533 and performed as a part of the ACCESS project consortium with direction from H. Yilmaz and O. Miersch-Wiemers, Robert Bosch, LLC. Recommended by Associate Editor U. Christen.

E. Hellström, J. Larimore, S. Jade, and A. G. Stefanopoulou are with the Department of Mechanical Engineering, University of Michigan, Ann Arbor, MI 48109 USA (e-mail: erikhe@umich.edu; larimore@umich.edu; sjade@umich.edu; annastef@umich.edu).

L. Jiang is with Robert Bosch LLC, Farmington Hills, MI 48331 USA (e-mail: li.jiang@us.bosch.com).

Color versions of one or more of the figures in this paper are available online at http://ieeexplore.ieee.org.

Digital Object Identifier 10.1109/TCST.2013.2271355

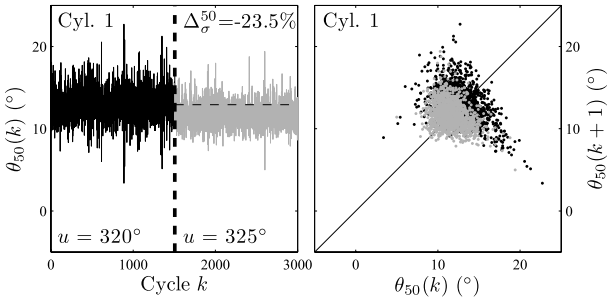

Fig. 1. Time series (left) and return maps (right) of combustion phasing. The constant start of injection, u, is set 5° earlier after half the time, which gives a dramatic reduction of the variability (the change in standard deviation, Δ_σ^{50}, is −23.5%). The aim here is to develop feedback controllers for the case when such steady-state solutions cannot be applied for reducing the variability.

Therefore, this brief aims to reduce CV through model-based control.

High CV in spark-ignition combustion, which is a related problem although the combustion process is clearly distinct from HCCI, was reduced in [6] by manipulating the injected fuel mass based on feedback from the crankshaft acceleration. Using injection during the negative valve overlap (NVO) period for the purpose of HCCI control is mentioned [1]. It was experimentally investigated in [7] for combustion mode transitions, in [8] for extending the lean limit, and in [9] and [10] for extending the low-load limit. Feedback control for reducing CV was developed in [11] using the injection timing. With the same objective, the valve timings were modified on a per-cycle basis in [12] and [13] and the injection quantity was modified in [14]. In contrast to the previous control works, the controllers are here augmented with integral action and a large number of cycles are used in the evaluation. Integral control enables the reduction of CV while regulating the mean combustion phasing at a point where the CV is high in open loop. A large dataset enables a quantitative statistical evaluation. Note that, because of the high sensitivity at the edge of stability, it is necessary to maintain the same nominal conditions when comparing open-loop and closed-loop operation. Specifically, the combustion phasing should on average be similar for the two cases. To illustrate, Fig. 1 shows open-loop data where the constant injection timing u is set 5° earlier[1] after half the experiment. This change advances the average combustion phasing only by 1.3° but reduces the standard deviation by 24%. Experiments have shown that it is typically trivial to reduce CV in steady state by phasing the combustion earlier through, for example, earlier injection

[1]The unit of u is degrees before top dead center combustion; see Fig. 2.

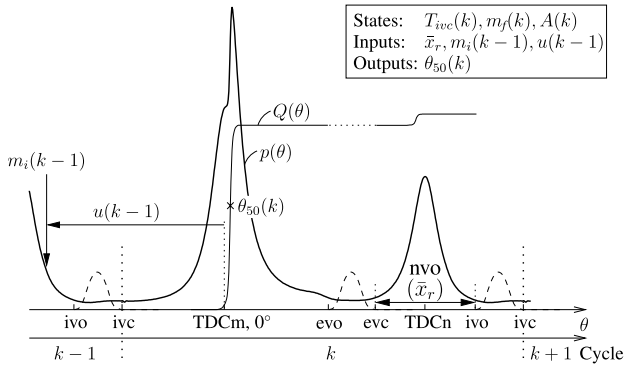

Fig. 2. Engine cycle and key variables for typical cylinder pressure $p(\theta)$, heat release $Q(\theta)$, and valve lift (dashed line). The states are the values at intake valve closing (IVC) for the temperature T_{ivc}, the fuel mass m_f, and the ignition scaling A. The inputs are the mean residual gas fraction $\bar{x}_r$, injection mass m_i, and injection timing u. The problem studied is to control $u(k)$ based on the feedback from the combustion phasing $\theta_{50}(k)$ with the goal to reduce CV.

timing, small increase in fuel mass, or earlier timing of the exhaust valve. The aim here is to control CV when such steady-state solutions do not apply. For example, if the combustion phasing is constrained to be late because of excessive pressure rise rates or during transients such as load transitions or combustion mode switches, when the combustion traverses regions with high CV. To approach this interesting and complex problem, this brief focuses on feedback control of the injection timing when other actuators are constant as a step toward handling transients also.

A physics-based model has recently been developed [15], [16] that predicts the dynamic evolution of the combustion phasing observed in single-cylinder experiments [17] for lean HCCI (with excess air) and with recycling of residual gas through NVO. Analysis of multicylinder experiments in [18] showed that the evolution in each cylinder was qualitatively similar and thus supported that the predicted characteristics were typical for these conditions. The model captures the deterministic coupling between cycles from the recycling of the thermal and chemical energy in the residual gas, and stochastic effects through random variations in the residual gas fraction. Stability analysis of the deterministic nonlinear dynamics shows that limit cycles and chaotic dynamics appear when reducing the residual gas fraction, and that runaway behavior appears for high residual gas fractions [16]. These characteristics, oscillatory dynamics and runaway behavior, are indeed observed in the experiments, and when the nonlinear deterministic model is driven with a stochastic input, the experimental observations at high CV are well captured. Model-based controllers for reducing CV were developed in [19] and evaluated by numerical simulation. The implementation of such controllers was reported in [20]. This brief is built based on these works and presents a model-based control design for reducing CV and evaluates the performance through experiments. This approach is used in combustion phasing feedback, calculated from cylinder pressure sensor data, to control the timing of the fuel injection during the NVO period.

This brief is organized as follows. The experimental setup is described first. Then follows a summary of the combustion model used for control design. The control problem is defined and discussed in Section IV and, after that, the controllers are designed and evaluated in experiments.

II. Experimental Setup

A four cylinder 2 L GM LNF Ecotec engine running premium grade indolene is used as the baseline platform. Modifications to accommodate HCCI combustion include increasing the compression ratio to 11.25:1 and using camshafts with shorter valve opening duration and reduced valve lift to allow for unthrottled operation. In addition to the stock turbocharger, the engine is augmented with a small supercharger (Eaton M24) to provide boost. Results presented here are run at slightly boosted conditions, ~ 1.1 bar intake manifold pressure, air–fuel ratio $\lambda \approx 1.2$, an engine speed of 1800 rpm and a load of approximately 3.25 bar net IMEP. Because the mixture is lean and highly diluted with internal residuals, the spark has negligible influence on the combustion. It is nevertheless left at a position of 40° after top dead center to prevent the spark plug from fouling.

Cylinder pressures are sampled at a resolution of 0.1°. For steady-state evaluation, a large number of cycles are recorded to accurately quantify the statistical properties. Therefore, 3000 consecutive engine cycles are recorded for each test, which is an order of magnitude more than is typical for engine dynamometer testing. Different levels of CV are achieved by trapping progressively less residuals through a retarding of the exhaust valve closing (EVC) time.

The control strategies are implemented using a combination of C and MATLAB code, and are tested in real-time using an ETAS ES910 rapid prototyping module. The feedback signal, the combustion phasing, is calculated by a Bosch electronic control unit connected to cylinder pressure sensors.

III. Combustion Model

The model presented in [15] and [16] captured the recycling of the thermal and chemical energy in the residual gas and utilized two states, namely the temperature, $T_{\text{ivc}}(k)$, at IVC and the fuel amount, $m_f(k)$, in the beginning of cycle k. The model considers that combustion efficiency varies with combustion phasing and that heat release occurs during both closed portions of the cycle. The inputs are the mean residual gas fraction, $\bar{x}_r$, and the injected fuel mass, $m_i(k)$. The model was extended in [19] to capture the effect of injection timing, denoted by u, by introducing an additional state, denoted by A, and in [20] with a burn duration model that better captured the experimental observations. The definition of the engine cycle and important variables in the model are shown in Fig. 2. In the following, the model from [15] and [16] with extensions from [19] and [20] was briefly summarized.

The structure of the complete model is

$$\begin{cases} T_{\text{ivc}}(k+1) = f_1\left(x(k), x_r(k)\right) \\ m_f(k+1) = f_2\left(x(k), x_r(k), m_i(k)\right) \\ A(k+1) = f_3\left(u(k)\right) \end{cases} \tag{1}$$

where $x(k) = \left(T_{\text{ivc}}(k), m_f(k), A(k)\right)$ is the state vector and $x_r(k)$ is the residual gas fraction. In practice x_r is regulated by

controlling the NVO and, as shown in [17], the NVO mainly influences the mean value, $\bar{x}_r$, while the variation around the mean was described by Gaussian white noise

$$x_r(k) = \bar{x}_r + e(k), \quad e(k) \in N(0, \sigma) \tag{2}$$

where $e(k)$ is normally distributed with zero mean and variance σ^2. One interpretation of (2) is that it approximates the lumped effect of higher order dynamics, such as turbulent flows, which affect the residual gas fraction in each cycle.

The temperature dynamics f_1, derived in [15] and [16], were

$$T_{\text{ivc}}(k+1) = (1 - x_r(k))T_{\text{im}} + x_r(k)T_r(k) \tag{3}$$

where the gas temperature at intake valve opening, $T_r(k)$, was

$$T_r(k) = \Bigg\{\alpha\left[1 + \beta\eta_m(\theta_m)m_f(k)V(\theta_m)^{\gamma-1}\right]^{\frac{1}{\gamma}} + \zeta m_f(k)(1 - \eta_m(\theta_m))\Bigg\}T_{\text{ivc}}(k) \tag{4}$$

and (α, β, ζ) are lumped parameters. The combustion efficiency, $\eta_m(\theta_m)$, is modeled by a sigmoid function. The end of main combustion $\theta_m(T_{\text{ivc}}(k), A(k))$ is given by

$$\theta_m = \theta_{\text{soc}} + \Delta\theta, \quad \Delta\theta = d_0 \exp\frac{\theta_{\text{soc}} - d_1}{d_2} \tag{5}$$

where the start of combustion is $\theta_{\text{soc}} = \kappa^{-1}(1)$

$$\kappa(\theta_{\text{soc}}, T_{\text{ivc}}, A) = \int_{\theta_{\text{ivc}}}^{\theta_{\text{soc}}} \frac{d\theta/\omega}{\tau(\theta, T_{\text{ivc}}, A)} \tag{6}$$

$\tau(\theta, T_{\text{ivc}}, A)$ is the ignition delay, and ω is the engine speed. The fuel dynamics f_2 are given by

$$m_f(k+1) = m_i(k) + x_r(k)\,(1 - \eta_m(\theta_m))\,(1 - \eta_n)\,m_f(k) \tag{7}$$

where η_n is the combustion efficiency during NVO, which is assumed constant. The function f_3 is introduced for the purpose of modeling the influence of the injection timing $u(k)$ on the ignition in the following cycle and is modeled by

$$A(k+1) = s_0 + s_1\left(1 + \exp\frac{s_2 - u(k)}{s_3}\right)^{-1} \tag{8}$$

where the injection timing $u(k)$ is given in crank angle degrees before top dead center combustion.

The output from the model is the combustion phasing, the 50% burn angle denoted by θ_{50}, which is approximated to occur after half the burn duration. Equation (5) then gives

$$\theta_{50}(k) = \theta_{\text{soc}}(k) + \frac{d_1}{2}\exp\frac{\theta_{\text{soc}}(k) - d_1}{d_2} \tag{9}$$

as the output equation.

A. Model Validation

The model parameters are calibrated with data from cylinder 1 in an operation point with fairly high CV. The models for the other cylinders are then generated by tuning one parameter, α in (4). Fig. 3 shows the return maps for the measurements and the predictions for the case used for calibration and another case with another valve timing, which give higher amounts of residual gas fraction and lower CV. The model predictions

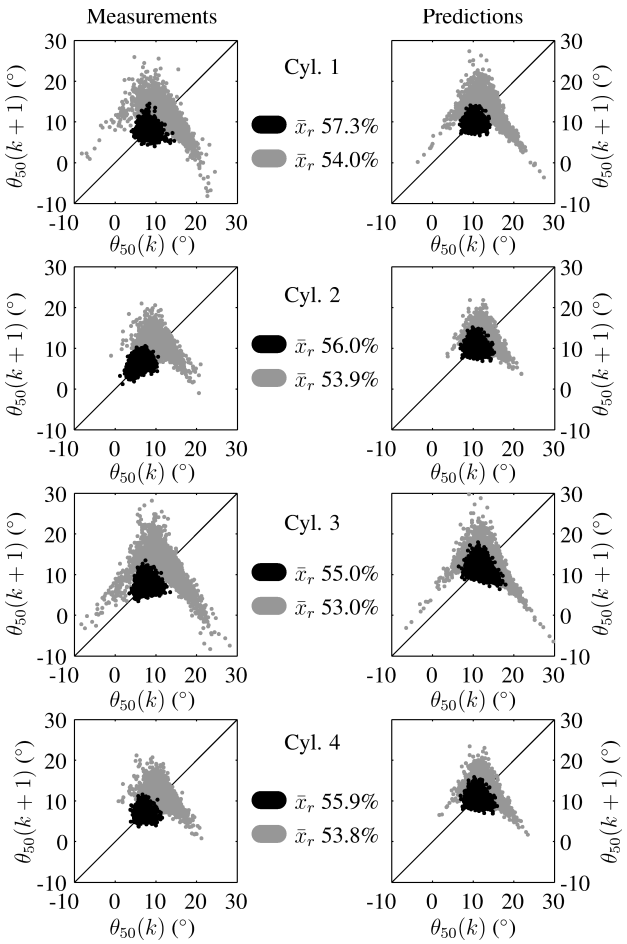

Fig. 3. Measured and predicted return maps for the combustion phasing θ_{50} in each cylinder for two different valve timings. The model captures the main characteristics of the cyclic variability and the variability between cylinders.

are on average slightly later, i.e., larger values of θ_{50}, than the measurements but capture the variability between cylinders and the dynamic cycle evolution fairly well when transitioning from low to high CV. The results here are for one engine speed and load. Future work aims to extend the model for the operating range of the engine.

IV. Control Problem

The inputs to the model in (1) are $\bar{x}_r$, m_i, and u. The residual gas fraction $\bar{x}_r$ is regulated by the NVO, as mentioned earlier, using commercially viable CAM phasing mechanisms. In general, and in the experimental setup here in particular, this control is on a considerably slower timescale than that of an engine cycle, and it is typically not possible to have cylinder-individual control. This is needed because of the variability between cylinders, see, Fig. 3. The injected fuel amount m_i is typically used to track the desired load from the driver. Control of $\bar{x}_r$ and m_i are thus limited by slow actuation and the requirement of tracking the desired load. Therefore, it is here assumed that these are constant and the problem of controlling the injection timing u for reducing the CV is studied. Note, however, that manipulating m_i on a per-cycle basis also gives the same or better performance and is beneficial if the authority

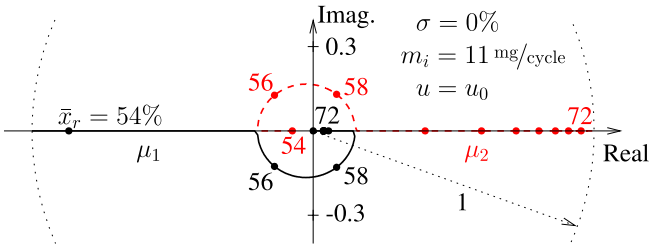

Fig. 4. Locus of the open-loop eigenvalues (μ_1, μ_2) for varying $\bar{x}_r$ between 53.7% (first period-doubling occurs) and 73.4% (runaway occurs).

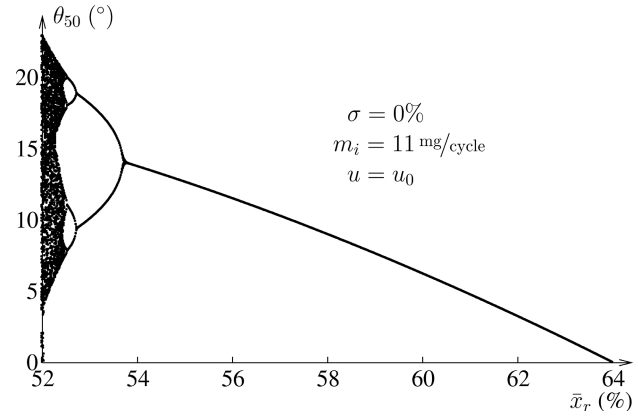

Fig. 5. Orbit diagram for the combustion phasing, θ_{50}, for the system in open loop.

of u is exhausted. Preliminary experiments with the control of both injection timing and quantity show that the variability in combustion phasing is slightly reduced but, at the same time, the variability in the torque increased. In summary, the model for the studied control problem is given by (1) and (2) as

$$\begin{cases} T_{\text{ivc}}(k+1) = g_1\left(T_{\text{ivc}}(k), m_f(k), A(k), \sigma\right) \\ m_f(k+1) = g_2\left(T_{\text{ivc}}(k), m_f(k), A(k), \sigma\right) \\ A(k+1) = g_3\left(u(k)\right) \end{cases} \tag{10}$$

where $(\bar{x}_r, m_i)$ are constant and externally specified parameters.

The feedback signal is the combustion phasing θ_{50}. This angle, calculated from in-cylinder pressure sensors, is a suitable signal to use in closed-loop control as shown in, e.g., [21]. For practical implementation, the controller also needs to be simple to make the computation of $u(k)$ based on the calculated $\theta_{50}(k)$—see Fig. 2—feasible in an on-board control unit.

A. Open-Loop Characteristics

The stability analysis in [16] of the open-loop characteristics, (10) with $u(k) = u_0$ and $\sigma = 0$, shows that the model is only stable for a range of residual gas fractions. This is shown in Fig. 4 that shows the eigenvalues (μ_1, μ_2) (the poles of the linearized system given by g_1 and g_2) for varying $\bar{x}_r$ for a constant load. For high amounts of residuals, runaway behavior occurs where the combustion phasing occurs increasingly earlier. For low amounts, a cascade of period-doubling bifurcations occurs, which eventually leads to seemingly chaotic behavior. These characteristics are shown in the orbit diagram in Fig. 5. Note that the orbit diagram shows the output (9) corresponding to stable fixed points or stable cycles for the model (10), when such exist. For $\bar{x}_r$ below 52.5%, there are no stable orbits and 100 iterations of the model are shown. It can finally be noted that, for the conditions studied here, noise levels around $\sigma = 1\%$ are typically observed in experiments. This is clearly significant considering the characteristics in Fig. 5.

V. Controller Design

Controller design for each cylinder based on the model in (10) is carried out for one operating point. The operating point corresponds to an engine speed of 1800 rpm, a load of 3.3 bar net IMEP corresponding to $m_i = [11]$ mg/cycle, an average residual gas fraction $\bar{x}_r = 54\%$, and an injection timing $u_0 = 330°$. These values are well-defined in an engine control unit (ECU) except for the residual gas fraction which is, as discussed earlier in Section III, described by random variations around the average value. The design is done in a deterministic setting, $\sigma = 0$, but the performance is evaluated for a range of $\bar{x}_r$ around the nominal value and with noise, $\sigma > 0$.

A. PI Control

Proportional feedback control is proposed in the first seminal papers on control of chaotic dynamics [22]–[24]. The controller design methods in these papers do not rely on an explicit model of the system, instead experimental observations are used to estimate a number of key features that determine the gain. Here, the model is utilized to select the gain. A proportional controller with feedback from the combustion phasing θ_{50} is

$$\delta u(k) = K_p(\theta_{50}(k) - \theta_{50}^*) \tag{11}$$

where K_p is the gain and θ_{50}^* is the desired reference point. To select the gain, the eigenvalues for the model (10) with $\bar{x}_r = 54\%$ and the control (11) are computed. From this locus of eigenvalues, the gain $K_p = 1.0$ is chosen to stabilize the system and reduce oscillatory behavior. Integral action is introduced by adding the term

$$K_i \sum_k (\theta_{50}(k) - \theta_{50}^*) T(k) \tag{12}$$

to the controller (11) where $T(k) = 120/N(k)$ is the time for one engine cycle at the speed N rpm. The gain K_i is chosen to slowly reach steady state with a time constant of 100 cycles, while not changing the transient response.

The performance of varying average residual gas fraction $\bar{x}_r$ is evaluated by computing the closed-loop eigenvalues of the linearized model. Fig. 6 shows the result for cylinder 1. The value of θ_{50}^* is set corresponding to the nominal point for the open-loop model. For $\bar{x}_r$ between 49% and 55%, the closed-loop dynamics are oscillatory but stable. Thus, the limit cycles and chaotic dynamics shown in Fig. 5 are stabilized and reduced to a stable fixed point. Outside the range shown

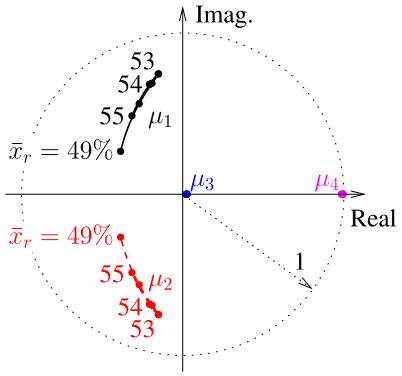

Fig. 6. Locus of eigenvalues with PI control is shown oscillatory but stable closed-loop dynamics for a range of residual gas fractions $\bar{x}_r$ (μ_4 is stable and, because of the slow integrator, rather insensitive to changes in gain and $\bar{x}_r$). The open-loop eigenvalues are shown in Fig. 4.

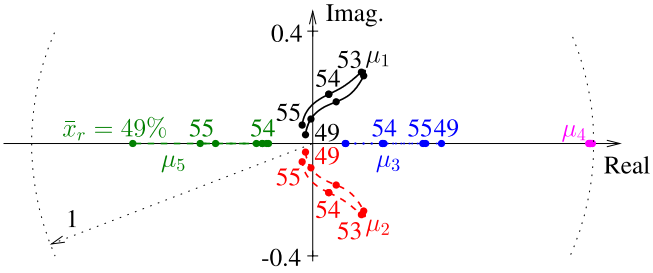

Fig. 7. Locus of eigenvalues with reduced-order LQG control for a range of residual gas fractions $\bar{x}_r$ (μ_4 is stable and is, because of the slow integrator, rather insensitive). The open-loop eigenvalues in this range are shown in Fig. 4.

in Fig. 5, the authority of the injection timing saturates and θ^*_{50} is not reached. The loci for the other cylinders are close and suggest similar behavior.

B. Reduced-Order LQG Control

To improve the transient response over PI control, an linear quadratic Gaussian (LQG) design is performed based on the linearized model. The Kalman filter is designed by setting the noise variance to 1 and the state covariance matrix diagonal with the elements 100, 1, and 10. For the regulator, the criteria $\sum_{k=1}^{\infty}\left(10\delta\theta_{50}(k)^2+\delta u(k)^2\right)$ is minimized. To simplify the controller as much as possible, controller order reduction is performed. The LQG regulator is composed of two lag compensators and one pole and zero that nearly cancels. By computing a balanced realization of the regulator and removing states with small Hankel singular values [25], a one-state regulator is obtained without any appreciable change in the magnitude and phase for all frequencies compared to the full-order regulator. The lag compensator stabilizes the system and to obtain zero steady-state error, integral action is introduced by (12), which does not have a significant influence on the transient response. The final reduced order controller is

$$C(z) = -1.13\frac{(z-1.04)(z+0.054)}{(z-1)(z-0.49)}. \tag{13}$$

Analogous to Fig. 6, the closed loop dynamics of the controller for cylinder 1 (the other cylinders exhibit similar behavior) are shown in Fig. 7 for varying $\bar{x}_r$. The closed-loop dynamics for $\bar{x}_r$ between 49% and 55% are stable, compare with the open loop in Figs. 4 and 5. Compared to PI control, the eigenvalue locations translate to oscillatory responses that are more damped if $\bar{x}_r$ is 50% or above.

VI. Experimental Results

The controllers are first evaluated in simulation using a noise level estimated from data, see [19]. After that, the controllers are implemented through rapid prototyping hardware coupled with engine instrumentation, actuators, and the ECU. The control signal, the injection timing u, is calculated on the rapid prototyping hardware while the feedback signal, the combustion phasing θ_{50}, is calculated in real-time by the ECU based on net heat release analysis of the cylinder pressure sensor data.

The objectives of the tests are to demonstrate the reduction of CV and to compare the effectiveness of different control schemes on various levels of CV. To minimize the variations in experiments because of environmental conditions, the tests presented here are performed consecutively allowing a fair comparison of the results to be drawn. Moreover, similar relative improvements are observed when repeating the tests on a day-to-day basis. The tests are run in open loop for approximately the first 1500 cycles while the controllers are active for the remaining 1500 cycles.

A. Comparison of Controllers

Each controller is run at three different EVC positions, the result being three values of residual gas fraction and CV. The value of the residual gas fraction is a complex function of the thermodynamics and flow conditions, and it is estimated by off-line pressure-based heat-release analysis [17], [26]. Because of the complexity, the estimated $\bar{x}_r$ changes for measurements are taken on different days even if the actuator settings are the same. Trends, however, such as later EVC gives less residuals and more CV, have been consistent. For these reasons, the absolute values for $\bar{x}_r$ during the controller evaluation differ from the values in the data used for model calibration and control design. The nominal case used for model calibration and the results shown in Sections III and IV, where $\bar{x}_r$ is 54% for cylinder 1, corresponds to the middle EVC position in the evaluation, where $\bar{x}_r$ is 51% for cylinder 1. Moreover, the variation in EVC spans a range of approximately 1% in $\bar{x}_r$. In conclusion, for the results in this section, the variation in the average residual gas fraction for the first cylinder corresponds approximately to $\bar{x}_r = 54\% \pm 1\%$ in Figs. 4–7.

A summary of the results is given in Table I. This table presents the mean combustion phasing for open and closed loop ($\bar{\theta}^{\mathrm{OL}}_{50}$, $\bar{\theta}^{\mathrm{CL}}_{50}$) and the open-loop standard deviation, $\sigma^{\mathrm{OL}}_{50}$. The effectiveness of the control is observed by the changes in standard deviation, which is denoted by Δ^{50}_{σ} and defined as negative when the control reduces the standard deviation.

The results in Table I show that both the controllers are effective in reducing the CV in all cases, although with

TABLE I
SUMMARY OF PI CONTROL (PI) AND REDUCED-ORDER LQG CONTROL (LQ) OF FOUR CYLINDERS WITH THREE LEVELS OF CV

	PI				LQ			
Cyl	$\bar{\theta}_{50}^{\mathrm{OL}}$	$\bar{\theta}_{50}^{\mathrm{CL}}$	$\sigma_{50}^{\mathrm{OL}}$	Δ_{σ}^{50}	$\bar{\theta}_{50}^{\mathrm{OL}}$	$\bar{\theta}_{50}^{\mathrm{CL}}$	$\sigma_{50}^{\mathrm{OL}}$	Δ_{σ}^{50}
evc = 102.5° aTDC								
1	11.0	10.5	1.9	-21.4	10.5	10.5	1.7	-4.7
2	10.8	10.5	2.1	-24.8	10.2	10.5	1.6	-0.3
3	10.8	10.5	1.9	-10.6	10.4	10.5	1.7	-0.5
4	10.3	10.5	1.6	-7.0	9.8	10.5	1.4	-12.1
evc = 101.5° aTDC								
1	11.6	11.0	2.1	-19.5	11.8	11.0	2.1	-11.9
2	11.1	11.0	2.2	-22.3	11.2	11.0	2.3	-19.4
3	11.2	11.0	2.2	-16.8	11.5	11.0	2.2	-17.3
4	11.1	11.0	2.0	-15.3	11.3	11.0	2.1	-20.2
evc = 100.5° aTDC								
1	12.2	11.8	2.6	-24.0	11.9	11.8	2.4	-16.4
2	11.7	11.8	3.2	-17.6	11.8	11.8	3.0	-15.8
3	11.8	11.8	2.6	-13.6	11.8	11.8	2.6	-1.2
4	11.6	11.8	2.4	-12.5	11.3	11.8	2.1	-4.3

varying performance. At low CV, there is less room for improvement, for lower residual gas fraction, and for higher CV, the physical limit for combustion is approached. As discussed earlier, the nominal case for the control design corresponds to a residual gas fraction of 51% in the control evaluation and, as expected, the controllers perform best at this operating point. The performance of the PI controllers, which have the same tuning for all cylinders, is robust for the variation in $\bar{x}_r$. The reduced-order LQG controllers, designed for the individual cylinders, perform well for the nominal point but are sensitive to deviations from this point. The full-order LQG regulator is also tested experimentally and does not offer improvements over the reduced-order regulator. The difference in robustness agrees with the higher bandwidth of the LQG controllers compared to the PI as well as the known possible loss of robustness of an LQ design when introducing a state estimator [27, Ch. 8.3].

It is observed that the integrator has effectively controlled the mean combustion phasing to the set point, which is chosen to make the difference from open loop small. It is also worth noting that reducing the standard deviation of θ_{50} typically gives a reduction in the coefficient of variation (CoV) of IMEP. Again, the PI performance is again similar for all cases while the LQG controllers only have a comparable performance for the nominal point. On average, the reduction in CoV Is 15% with the PI controller and 4% with the reduced-order LQG controller.

Figs. 8 and 9 show the results of cylinders 1 and 2 through the probability density plot for the return map of the combustion phasing. A return map shows the relationship between the consecutive cycles of a variable, here the combustion phasing θ_{50} in cycle k versus in cycle $k+1$, which provides insight into the dynamic behavior. The probability density $p(\theta_{50}(k), \theta_{50}(k+1))$ shows the probability for a transition from $\theta_{50}(k)$ to $\theta_{50}(k+1)$. When the variability is low, the

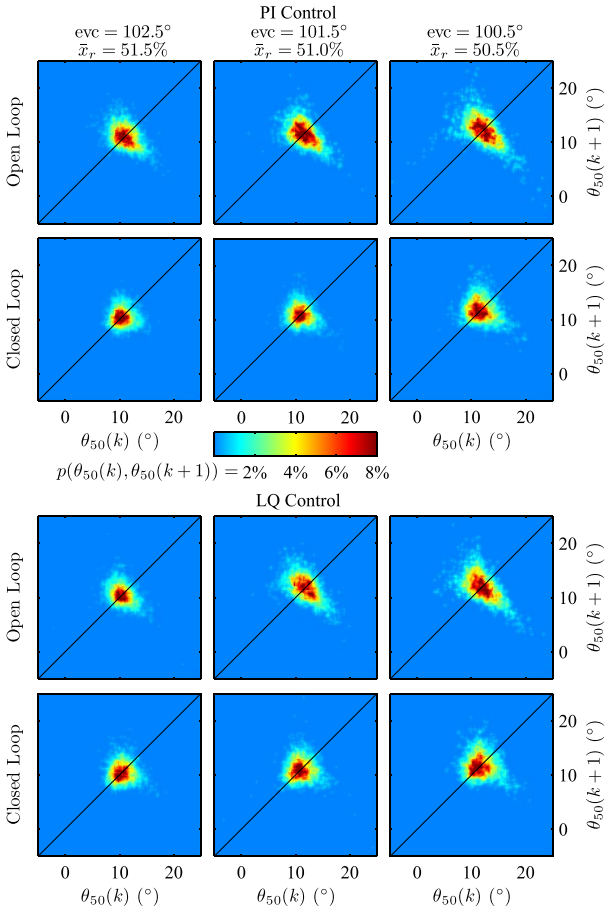

Fig. 8. Probability density plots for the evolution of combustion phasing θ_{50} in cylinder 1 for open and closed loop with the respective controller. The density concentration on the diagonal indicates effective control.

phasing in cycle k should not deviate much from the phasing in cycle $k+1$ and should therefore always return to a similar value, which means that the return map contracts and the probability density increases close to the point $\theta_{50}(k) = \theta_{50}(k+1)$ on the diagonal. The figures show that the controllers are effective in contracting the return map by concentrating the distribution and the effect is more pronounced when the open loop case has higher CV.

B. Evaluation of Control Effectiveness

Fig. 10 shows the time series data of combustion phasing and the control signal, the injection timing u, for cylinders 1 and 2. The results shown are for the PI control with the middle EVC position in Table I. There is a visible reduction in the variability of the combustion when transitioning from open loop (gray) to closed loop (black). In addition, the control perturbations are small, less than $\pm 5°$, and the reduction is achieved while maintaining the perturbation around the open loop value of u.

Symbolic statistics for the PI and reduced-order LQG control are displayed in Fig. 11. Symbolic statistics is a nonlinear time series technique used to quantify the probability that sequences of cycles occur, for a detailed explanation, see [18] and [28]. Following [18], the sequence length is set

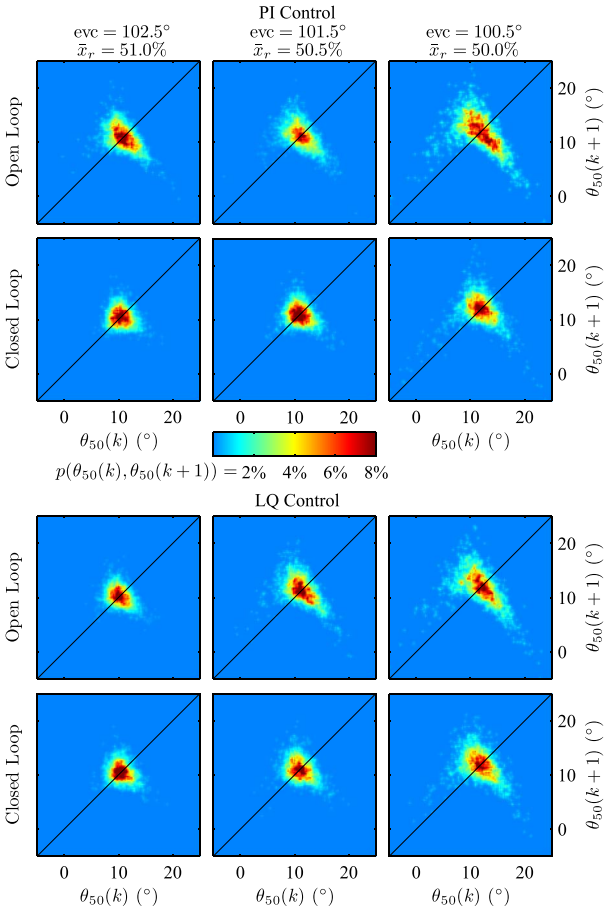

Fig. 9. Probability density plots for the evolution of the combustion phasing θ_{50} in cylinder 2 for open and closed loop with the respective controller. The density concentration on the diagonal indicates effective control.

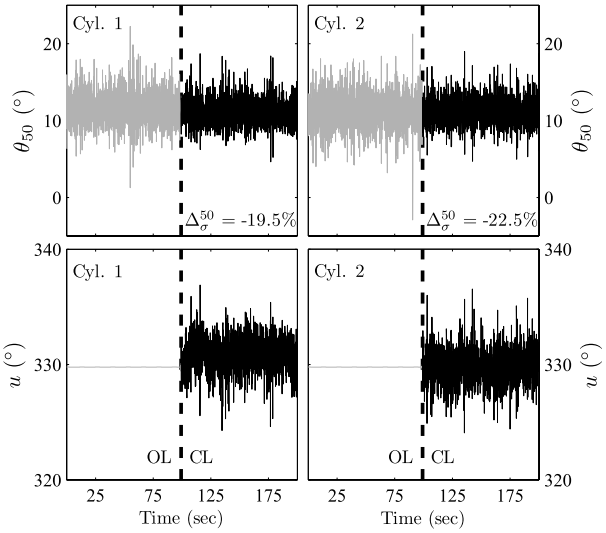

Fig. 10. PI control with the middle EVC position. Open-loop results in gray and closed loop in black show the reduction in combustion phasing variability (top) and the injection timing control signal u (bottom).

to three ($L = 3$) and the times series data are divided into five bins ($n = 5$) where each bin represents a symbol. The bin intervals are chosen such that each symbol is equally probable,

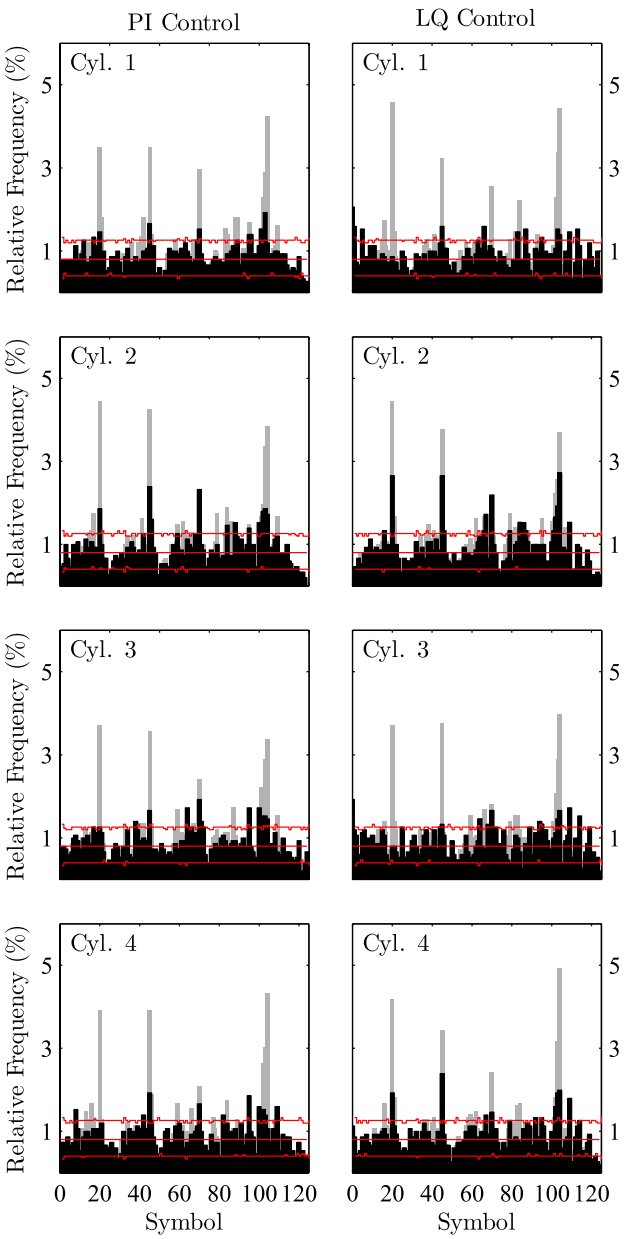

Fig. 11. Symbolic statistics of PI control (PI) and reduced-order LQG control (LQ) for the middle EVC position. Open loop is in gray and closed loop in black. The lines are the equally probable lines with 95% confidence intervals. The flattening of the symbolic statistics indicates effective control.

which means that if the dynamic evolution is purely random each sequence should be equally probable. Without strong deterministic couplings between the cycles, the histogram for all sequences of symbols should thus be flat and close to the $n^{-L} = 0.8\%$ line. The 95% confidence intervals for the line are computed from 100 shuffled surrogates obtained by randomly reordering data; see [28]. The equally probable line and confidence intervals are shown with solid lines in the symbol-sequence histograms in Fig. 11. For combustion with low variability, the histograms are rather flat, indicating random evolution, while for high variability, a number of sequences appear with significant probability; see [18]. With control, the deterministic couplings between the cycles should ideally disappear, leaving only random noise in the output.

For cylinders 1 and 3, both the controllers almost bring the statistics within the confidence intervals indicating that mostly random noise remains. The results of the other cylinders show that there are still deterministic couplings between cycles, although the probability for the sequence characteristics for high CV occurring is clearly reduced.

VII. Conclusion

Model-based design of feedback controllers for reducing CV in lean autoignition combustion was presented. The controllers were evaluated in experiments on a multicylinder engine. The timing of the fuel injection event was controlled using feedback from the combustion phasing, calculated the ECU onboard using cylinder pressure data. It was demonstrated that, because of high sensitivity at the edge of stable operation, integral action that maintains an average combustion phasing was required for a proper evaluation of the controller performance. A PI controller performed well for an operating point (engine, speed, and load) for various levels of residual gas fraction, which gave various levels of CV in open loop. The combustion model was important for the calibration because of stochastic nature of the problem. The PI control had more robust performance than LQG controllers, designed for the individual cylinders, and reduced the standard deviation in combustion phasing for all cylinders between 7%, 25%, and 17% on average. This was translated into a 15% average reduction in the coefficient of variation of IMEP. The successful results motivated further work on model-based control for reducing CV in, e.g., late phasing operation because of pressure rise rate constraints, load transitions, and combustion mode switches.

Acknowledgment

The authors would like to thank J. Sterniak and J. Vanier for their help in experimental hardware and software.

References

[1] J. Willand, R.-G. Nieberding, G. Vent, and C. Enderle, "The knocking syndrome—Its cure and its potential," in *Proc. SAE Int. Fall Fuels Lubricants Meeting Exhibit.*, Oct. 1998.

[2] L. Koopmans and I. Denbratt, "A four stroke camless engine, operated in homogeneous charge compression ignition mode with commercial gasoline," in *Proc. SAE World Congr.*, Sep. 2001.

[3] L. Manofsky, J. Vavra, D. Assanis, and A. Babajimopoulos, "Bridging the gap between HCCI and SI: Spark-assisted compression ignition," in *Proc. SAE World Congr.*, Apr. 2011.

[4] C. J. Chiang and A. G. Stefanopoulou, "Stability analysis in homogeneous charge compression ignition (HCCI) engines with high dilution," *IEEE Trans. Control Syst. Technol.*, vol. 15, no. 2, pp. 209–219, Mar. 2007.

[5] S. Jade, J. Larimore, E. Hellström, L. Jiang, and A. G. Stefanopoulou, "Enabling large load transitions on multicylinder recompression HCCI engines using fuel governors," in *Proc. Amer. Control Conf.*, 2013.

[6] L. I. Davis, Jr., L. A. Feldkamp, J. W. Hoard, F. Yuan, F. T. Connolly, C. S. Daw, and J. B. Green, Jr., "Controlling cyclic combustion variations in lean-fueled spark-ignition engines," in *Proc. SAE World Congr.*, 2001.

[7] L. Koopmans, H. Ström, S. Lundgren, O. Backlund, and I. Denbratt, "Demonstrating a SI-HCCI-SI mode change on a Volvo 5-cylinder electronic valve control engine," in *Proc. SAE World Congr.*, 2003.

[8] T. Urushihara, K. Hiraya, A. Kakuhou, and T. Itoh, "Expansion of HCCI operating region by the combination of direct fuel injection, negative valve overlap and internal fuel reformation," in *Proc. SAE World Congr.*, 2003.

[9] H. Song, A. Padmanabhan, N. B. Kaahaaina, and C. Edwards, "Experimental study of recompression reaction for low-load operation in direct-injection homogeneous charge compression ignition engines with n-heptane and i-octane fuels," *Int. J. Eng. Res.*, vol. 10, no. 4, pp. 215–229, Aug. 2009.

[10] N. Wermuth, H. Yun, and P. Najt, "Enhancing light load HCCI combustion in a direct injection gasoline engine by fuel reforming during recompression," *SAE Int. J. Eng.*, vol. 2, no. 1, pp. 823–836, Apr. 2009.

[11] A. F. Jungkunz, H.-H. Liao, N. Ravi, and J. C. Gerdes, "Combustion phasing variation reduction for late-phasing HCCI through cycle-to-cycle pilot injection timing control," in *Proc. ASME Dyn. Syst. Control Conf.*, 2011.

[12] N. Ravi, M. J. Roelle, H.-H. Liao, A. F. Jungkunz, C.-F. Chang, S. Park, and J. C. Gerdes, "Model-based control of HCCI engines using exhaust recompression," *IEEE Trans. Control Syst. Technol.*, vol. 18, no. 6, pp. 1289–1302, Nov. 2010.

[13] A. F. Jungkunz, H.-H. Liao, N. Ravi, and J. C. Gerdes, "Reducing combustion variation of late-phasing HCCI with cycle-to-cycle exhaust valve timing control," in *Proc. IFAC Symp. Adv. Autom. Control*, 2010, pp. 815–820.

[14] A. F. Jungkunz, S. Erlien, and J. C. Gerdes, "Late phasing homogeneous charge compression ignition cycle-to-cycle combustion timing control with fuel quantity input," in *Proc. Amer. Control Conf.*, 2012, pp. 2078–2083.

[15] E. Hellström and A. G. Stefanopoulou, "Modeling cyclic dispersion in autoignition combustion," in *Proc. 50th IEEE Conf. Decision Control*, Dec. 2011, pp. 6834–6839.

[16] E. Hellström, A. G. Stefanopoulou, and L. Jiang, "Cyclic variability and dynamical instabilities in autoignition engines with high residuals," *IEEE Trans. Control Syst. Technol.* [Online]. Available: http://dx.doi.org/10.1109/TCST.2012.2221715

[17] E. Hellström, A. G. Stefanopoulou, J. Vávra, A. Babajimopoulos, D. Assanis, L. Jiang, and H. Yilmaz, "Understanding the dynamic evolution of cyclic variability at the operating limits of HCCI engines with negative valve overlap," *SAE Int. J. Eng.*, vol. 5, no. 3, pp. 995–1008, 2012.

[18] E. Hellström, J. Larimore, A. G. Stefanopoulou, J. Sterniak, and L. Jiang, "Quantifying cyclic variability in a multicylinder HCCI engine with high residuals," *J. Eng. Gas Turbines Power*, vol. 134, no. 11, p. 112803, 2012.

[19] E. Hellström, A. G. Stefanopoulou, and L. Jiang, "Reducing cyclic dispersion in autoignition combustion by controlling fuel injection timing," in *Proc. 51st IEEE Conf. Decision Control*, Dec. 2012, pp. 3747–3752.

[20] J. Larimore, E. Hellström, S. Jade, L. Jiang, and A. G. Stefanopoulou, "Controlling combustion phasing variability with fuel injection timing in a multicylinder HCCI engine," in *Proc. Amer. Control Conf.*, 2013, pp. 1–6.

[21] J. Bengtsson, P. Strandh, R. Johansson, P. Tunestål, and B. Johansson, "Closed-loop combustion control of homogeneous charge compression ignition (HCCI) engine dynamics," *Int. J. Adapt. Control Signal Process.*, vol. 18, no. 2, pp. 167–179, 2004.

[22] E. Ott, C. Grebogi, and J. A. Yorke, "Controlling chaos," *Phys. Rev. Lett.*, vol. 64, no. 11, pp. 1196–1200, 1990.

[23] B. Peng, V. Petrov, and K. Showalter, "Controlling chemical chaos," *J. Phys. Chem.*, vol. 95, no. 13, pp. 4957–4959, 1991.

[24] V. Petrov, V. Gaspar, J. Masere, and K. Showalter, "Controlling chaos in the Belousov–Zhabotinsky reaction," *Nature*, vol. 361, no. 6409, pp. 240–243, Jan. 1993.

[25] B. D. O. Anderson and Y. Liu, "Controller reduction: Concepts and approaches," *IEEE Trans. Autom. Control*, vol. 34, no. 8, pp. 802–812, Aug. 1989.

[26] J. Larimore, E. Hellström, J. Sterniak, L. Jiang, and A. G. Stefanopoulou, "Experiments and analysis of high cyclic variability at the operational limits of spark-assisted HCCI combustion," in *Proc. Amer. Control Conf.*, Jun. 2012, pp. 2072–2077.

[27] B. D. O. Anderson and J. B. Moore, *Optimal Control: Linear Quadratic Methods*. Englewood Cliffs, NJ, USA: Prentice-Hall, 1990.

[28] C. E. A. Finney, J. B. Green, Jr., and C. S. Daw, "Symbolic time-series analysis of engine combustion measurements," in *Proc. SAE World Congr.*, 1998.